Fixed Subset Selection to Reduce Advanced RAIM Complexity

Juan Blanch, Todd Walter, Per Enge

Stanford University

ABSTRACT

Advanced RAIM has the potential of achieving global coverage of vertical guidance, even with large probabilities of satellite fault. To achieve this performance, airborne receivers will need to take into account a large number of fault modes resulting from the combination of single satellite and single constellation faults. Baseline implementations of ARAIM require the computation of a subset position solution (or at least the associated error covariance) per fault mode, which can result in a large computational burden. Consolidating the fault modes can reduce the list of subsets very significantly. This paper proposes to use a fixed set of subsets for a dual constellation configuration. This approach has two advantages: it simplifies the algorithm (the list of subsets is no longer dynamic), and it reduces the computational load. For a baseline GPS – Galileo configuration, the number of subsets is reduced from several thousands to less than seventy with a minimal impact on availability.

INTRODUCTION

Advanced RAIM [1] is a proposed extension of RAIM to dual frequency and multi-constellation GNSS that could initially enhance horizontal guidance coverage and eventually deliver global coverage of vertical guidance. In order to achieve this performance, airborne receivers will need to track two or three times more satellites than current receivers, and one more signal per satellite (L5). In addition, compared to RAIM, more fault modes will need to be taken into account. This is due to three factors: the increased criticality of vertical guidance operations, the increased number of satellites, and the fact that new constellations may have higher fault probabilities of fault.

The reference ARAIM airborne algorithm described in [1] proposes a method to determine the list of fault modes that need to be monitored. Then, for each of these fault modes, a subset solution is computed and compared to the all-in-view solution. The list of fault modes is dependent on the probabilities of satellite fault and constellation fault P_{sat} and P_{const} (which are specified in the Integrity Support Message). In addition to being dynamic, this list can become long for large values of P_{sat} and P_{const}. These two potential downsides could hinder the development of ARAIM.

There are several methods to reduce ARAIM complexity. One way consists in performing satellite selection: the receiver only uses a subset of all the satellites that are in view [2], [3]. This approach reduces the overall receiver computational load for any GNSS based system, and reduces the number of subsets for ARAIM. Another way of reducing the load, and one that is more specific to ARAIM, is fault consolidation [4], [5], [6], [7], [8]. The idea of fault consolidation is to group faults so that one subset solution can monitor multiple faults. These proposed methods significantly reduce the number of subsets. However, except for [2], which only covers a very specific configuration, the list of subsets is dynamic, that is, it is dependent on the values of P_{const} and P_{sat}.

The goal of this paper is to further simplify the subset selection, while maintaining an acceptable performance. In the first part, we provide upper bounds on the number of subset solutions that are computed in the reference algorithm described in [1] as a function of the Integrity Support Message parameters P_{sat} and P_{const}, and the number of satellites. The results will be presented as tables showing the number of subsets that the receiver needs to compute as a function of P_{sat}, P_{const} and the number of satellites. In the second part, we propose a method to reduce the number of subset based on fault consolidation. More specifically, we propose a set of simple schemes with a fixed subset selection (with fewer than 70 subsets), independent of P_{sat} and P_{const}. Finally we evaluate and compare the proposed schemes to the reference ARAIM algorithm using availability simulations in representative scenarios.

COMPUTATIONAL LOAD OF THE WG-C REFERENCE ARAIM ALGORITHM

The computational load is going to be very dependent on the details of the implementation of the algorithm. For example, exploiting the structure of the subsets using rank one updates can lead to significant computation savings. However, even exploiting this structure, the complexity of the algorithm will be approximately linear in the number of subsets. For this reason, the number of subsets that the algorithm monitors is a useful measure of the complexity.

Figure 1 shows the number of subsets that is monitored as a function of P_{sat} for a geometry with two constellations with ten satellites each and a P_{const} fixed at 10^{-4}. The number of subsets remains below a hundred for a P_{sat} of 10^{-5} (the algorithm checks each single fault and the two constellation wide faults). For values around 10^{-4}, this number reaches multiple hundreds, and it is in the thousands for 10^{-3}. While the length of these lists is not problematic in simulation or prototype settings, it is likely to be prohibitive for certified airborne receivers.

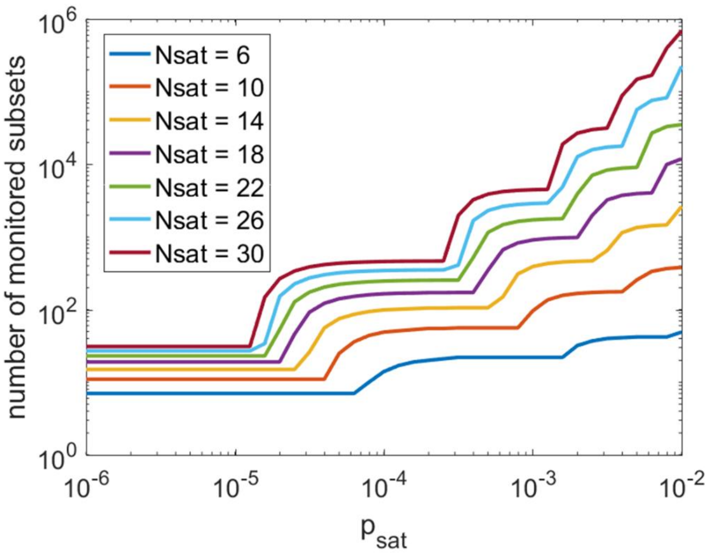

Figure 1. *Number of subsets as a function of P_{sat}.*

Note that the number of subsets is also dependent on the allocation (noted P_THRES in the algorithm description [1]) that is given to the fault modes that are not monitored. However, the number of subsets is weakly dependent on this parameter for any practical choice.

LIST OF SUBSETS FOR TWO CONSTELLATIONS

We propose three types of subsets in addition to the all-in-view: single satellite out, one constellation out, and one constellation out plus one single satellite. In the next paragraphs, we specify which fault modes are covered by each subset and provide the probability associated with it.

Notations:

$P_{sat,i}^{(j)}$: probability of fault in satellite *i* from constellation *j*

$P_{const,j}$: probability of constellation fault in constellation *j*

$N_{sat,j}$: number of satellites in constellation *j*

Single satellite out

Each of these subsets corresponds to a fault in one satellite and one satellite only. We have:

$$P^{(j)}_{\text{single\_satellite},i} = \frac{P^{(j)}_{sat,i}}{1-P^{(j)}_{sat,i}} P^{(1)}_{no\_fault} P^{(2)}_{no\_fault} \tag{1}$$

where:

$$P^{(j)}_{no\_fault} = \left(1-P_{const,j}\right) \prod_{k=1}^{N^{(j)}_{sat}} \left(1-P^{(j)}_{sat,k}\right) \tag{2}$$

There are N_{sat} such subsets. A simple upper bound (and very good approximation) is given by:

$$P^{(j)}_{\text{single\_satellite},i} = P^{(j)}_{sat,i} \tag{3}$$

Single constellation out

Each of these subsets corresponds to no fault in one constellation, and a constellation fault or two and more simultaneous faults in the other one:

$$P_{\text{single\_constellation},j} = \frac{P_{const,j}}{1-P_{const,j}} \frac{P_{no\_fault}}{1-P_{no\_fault,j}} + \left(1-P_{no\_fault,j} - P_{no\_fault,j} \sum_{i=1}^{N_{sat,j}} \frac{P^{(j)}_{sat,i}}{1-P^{(j)}_{sat,i}}\right) \frac{P_{no\_fault}}{1-P_{no\_fault,j}} \tag{4}$$

where $P_{no\_fault} = P_{no\_fault,1} P_{no\_fault,2}$

The first term corresponds to the constellation fault, and the second one corresponds to two or more simultaneous faults. The second term is obtained by observing that the probability of two or more faults is the total probability (one) minus the probability of no fault or exactly one fault. There are two such subsets.

This probability is bounded and well approximated by:

$$P_{\text{single\_constellation},j} = P_{const,j} + \frac{1}{2}\left\{\left(\sum_{i=1}^{N_{sat,j}} P^{(j)}_{sat,i}\right)^2 - \sum_{i=1}^{N_{sat,j}} P^{(j)2}_{sat,i}\right\} \tag{5}$$

The proof for the second term is shown in the Appendix.

Single constellation out and single satellite out

Each of these subsets corresponds to one fault or more in constellation 1 and one single satellite fault in constellation 2:

$$P_{\text{single\_sat},i\text{\_single\_constellation},1} = P_{no\_fault,2} \frac{P_{sat,i}^{(2)}}{1-P_{sat,i}^{(2)}} \left(1-P_{no\_fault,1}\right) \tag{6}$$

This probability is bounded and well approximated by:

$$P_{\text{single\_sat},i\text{\_single\_constellation},1} = P_{sat,i}^{(2)} \left(P_{const,1} + \sum_{i=1}^{N_{sat,1}} P_{sat,i}^{(1)} \right) \tag{7}$$

For the other constellation, these subsets correspond to two satellite faults or more or a constellation fault in constellation 2 and one single satellite fault in the other one. The probability associated with it is:

$$P_{\text{single\_sat},i\text{\_single\_constellation},2} = P_{no\_fault,1} \frac{P_{sat,i}^{(1)}}{1-P_{sat,i}^{(1)}} \left(1 - P_{no\_fault,2} - P_{no\_fault,2} \sum_{i=1}^{N_{sat,2}} \frac{P_{sat,i}^{(2)}}{1-P_{sat,i}^{(2)}} \right) \tag{8}$$

It can be bounded and approximated by:

$$P_{\text{single\_sat},i\text{\_single\_constellation},2} = P_{sat,i}^{(1)} \left[P_{const,2} + \frac{1}{2} \left\{ \left(\sum_{i=1}^{N_{sat,2}} P_{sat,i}^{(2)} \right)^2 - \sum_{i=1}^{N_{sat,2}} P_{sat,i}^{(2)2} \right\} \right] \tag{9}$$

Equations (8) and (9) are obtained using the methods used for Equations (4) and (5). We note that there is an asymmetry in the probabilities expressed in Equations (7) and (9). This is due to the fact that the fault modes composed of a single satellite fault in each constellation can be accounted in either the first set or the second set. As written above, they are accounted in the first set. In the simulations below, constellation 1 is the constellation with the highest number of satellites in view.

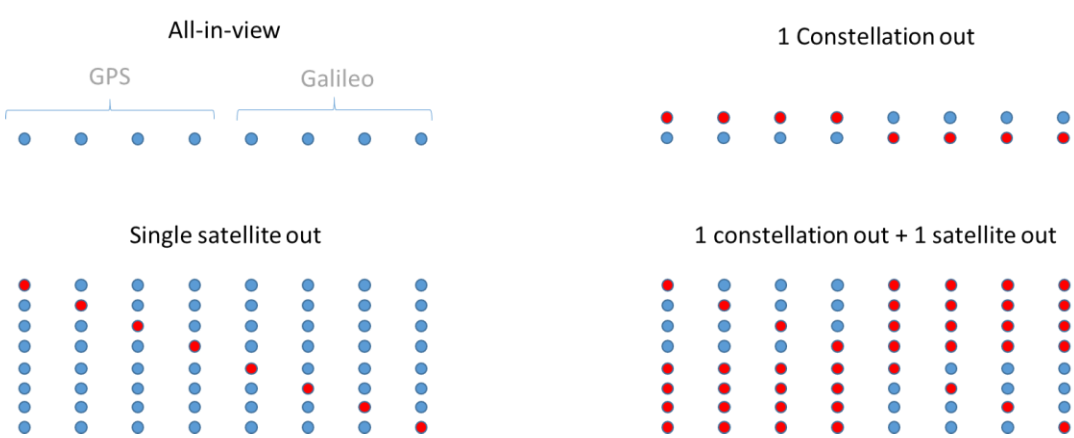

Figure 2. *List of subsets formed by the receiver. Each row is a subset where the blue dots represent satellites that are included and the red dots are satellites that are excluded*

By inspection, it can be verified that all the following combinations are accounted for:

- Any combination of faults in one constellation and none in the other one
- At least one fault in one constellation (wide or narrow) and one satellite fault in the other

Fault modes that are not monitored

The following fault modes are not monitored:

- all faults modes composed of four or more primary faults (constellation or satellite fault)
- two simultaneous constellation faults
- one constellation fault and two or more faults in the other constellation

An upper bound is given by:

$$P_{not\_monitored} = \frac{1}{24}\left(P_{const,1} + P_{const,2} + \sum_i P_{sat,i}^{(1)} + \sum_i P_{sat,i}^{(1)}\right)^4 + P_{const,1}P_{const,2} + \frac{1}{2}P_{const,1}\left[\left(\sum_i P_{sat,i}^{(2)}\right)^2 - \sum_i P_{sat,i}^{(2)2}\right] + \frac{1}{2}P_{const,2}\left[\left(\sum_i P_{sat,i}^{(1)}\right)^2 - \sum_i P_{sat,i}^{(1)2}\right] \quad (10)$$

It can be verified that for P_{const} smaller than 10^{-4} and P_{sat} smaller than 10^{-3}, we have $P_{not\_monitored} < 10^{-7}$ as long as the number of satellites in each constellation is smaller than 17. Table 1 shows how all the fault modes are taken into account by the list of subsets and $P_{not\_monitored}$.

constellation 1/ constellation 2	No fault	1 satellite fault only in constellation 1	2 satellite faults or more in constellation 1	constellation fault in 1
No fault	All-in-view	Single sat. in 1 out	Single const. 1 out	Single const. 1 out
1 satellite fault only in constellation 2	Single sat. in 2 out	Single sat. in 1/2 out + single const. 2/1 out or	Single sat. in 2 + single const. 1	Single sat. in 2 + single const. 1
2 satellite faults or more in constellation 2	Single const. 2 out	Single sat. in 1 out + single const. 2 out	Not monitored (first term in Eq.(10))	Not monitored (third term in Eq.(10))
Constellation fault	Single const. 2 out	Single sat. out + single const. 2 out	Not monitored (fourth term in Eq. (10))	Not monitored (second term in Eq. (10))

Table 1. *Mapping of fault modes to subsets*

COMPARISON BETWEEN BASELINE ALGORITHM AND PROPOSED SCHEME

In this section we compare the performance of the subset selection proposed here with the one defined in the baseline algorithm as defined in [9], which is an evolution of the algorithm described in [1]. The rest of the algorithm is not modified. We simulate the performance of dual frequency GPS-Galileo ARAIM using the error models and baseline constellation configuration (GPS 24 – Galileo 24) described in [1]. The user settings are:

- 10 by 10 degree user grid
- 24 hours
- 300 s time steps

The URA/SISA was set at 1 m, the URE at 0.66 m, and P_{const} at 10^{-4}. Figures 3 through 8 show results for $P_{sat} = 10^{-4}$ and $P_{sat} = 10^{-3}$. For $P_{sat} = 10^{-4}$, even though a small degradation in coverage can be observed (from 97.95% to 94.69%), the coverage is still good. Figure 5 shows how the fixed subsets affect the VPLs. For most geometries (the strong ones), the VPLs are actually reduced. This is due to the reduction in the test statistics resulting from the increased probability of false alert per mode. For a minority of geometries, the VPL increases because of the loss of geometry strength resulting from the subset consolidation. It is these geometries that drive the small degradation in coverage. For $P_{sat}=10^{-3}$ (Figures 6,7 and 8), it is the second effect that drives the performance: the coverage improves with the fixed list of subset.

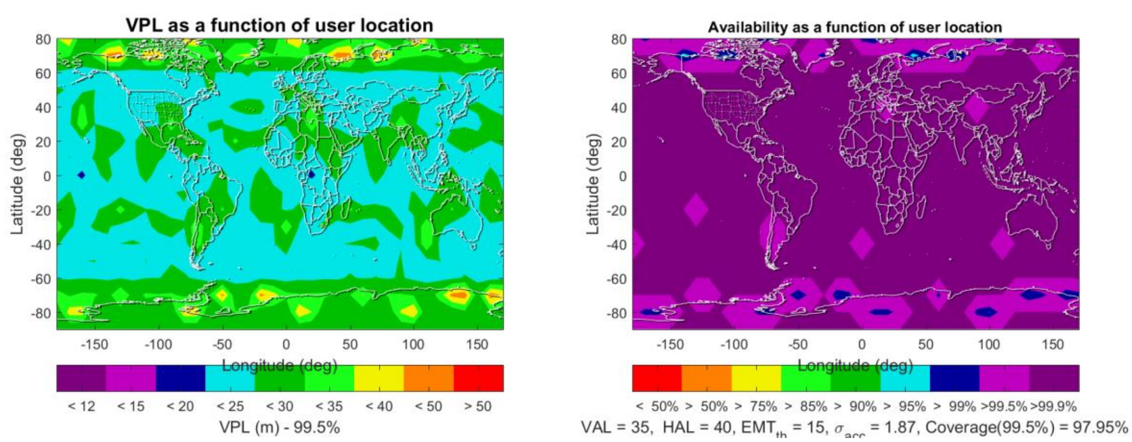

Figure 3. *99.5% VPL percentile and LPV-200 availability for $P_{sat} = 10^{-4}$ for the baseline algorithm.*

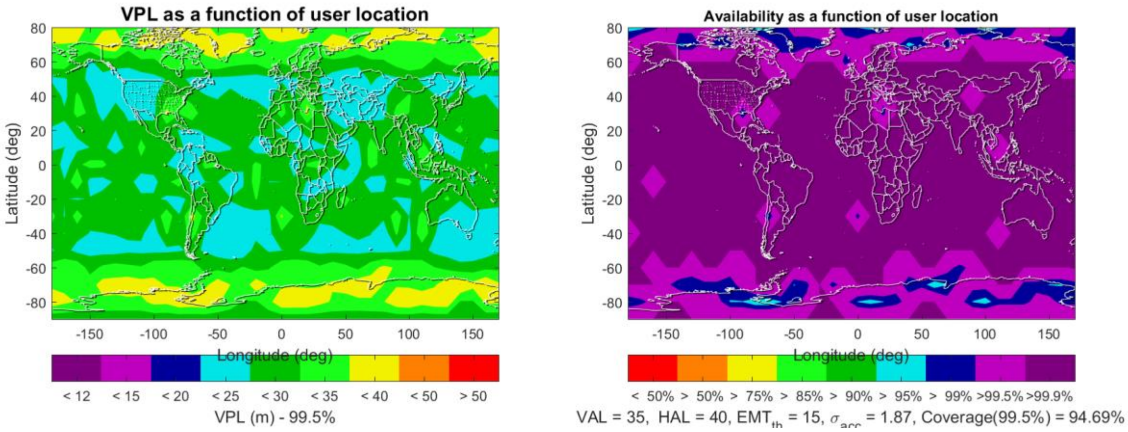

Figure 4. *99.5% VPL percentile and LPV-200 availability for $P_{sat} = 10^{-4}$ with the fixed subset list.*

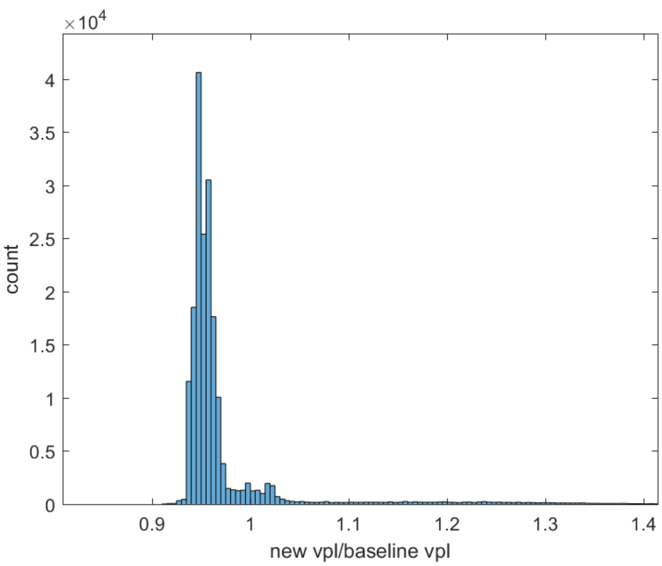

Figure 5. *Histogram of the ratio of the fixed list VPL to the baseline VPL for $P_{sat} = 10^{-4}$*

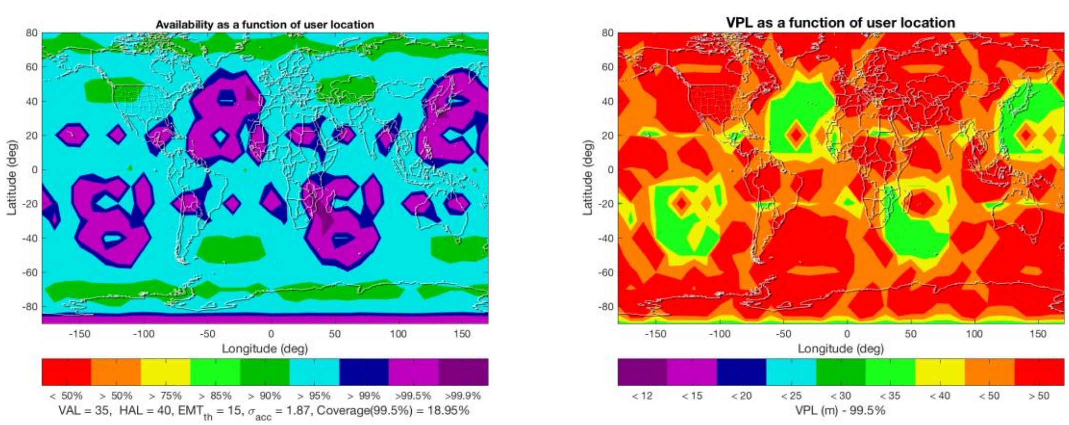

Figure 5. *99.5% VPL percentile and LPV-200 availability for P_{sat} = 10^{-3} for the baseline algorithm.*

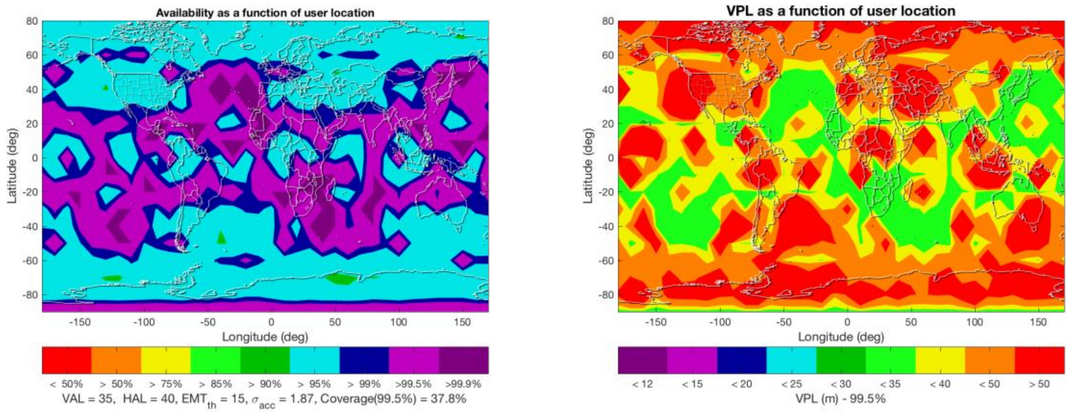

Figure 6. *99.5% VPL percentile and LPV-200 availability for P_{sat} = 10^{-3} with the fixed subset list.*

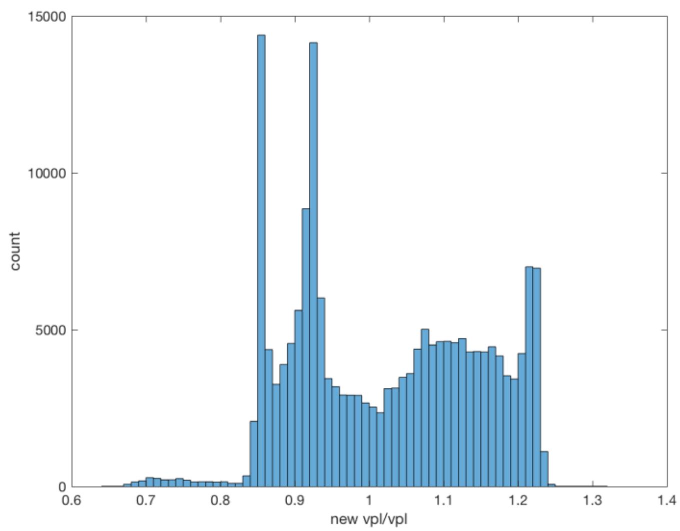

Figure 7. *Histogram of the ratio of the fixed list VPL to the baseline VPL for P_{sat} = 10^{-3}*

COMPUTATIONAL REDUCTION

As indicated earlier, the computational load is very dependent on the specific implementation of the algorithm (and in particular on whether the structure of the problem is exploited), but it is expected to be approximately proportional to the length of the subset list. Table 2 shows the number of subsets for the baseline algorithm and for the proposed fixed list as a function of the number of satellites. For the baseline algorithm, these numbers were computed assuming an equal number of satellites in each constellation and maximum total probability of not monitored fault modes of $6x10^{-8}$.

N_{sat}	8	12	16	20	24	28	32
Baseline with $P_{sat} = 10^{-4}$	49	81	100	144	196	256	324
Baseline with $P_{sat} = 10^{-3}$	128	248	604	1134	1950	3266	5034
Fixed list	23	31	35	43	51	59	67

Table 2. *Number of subsets for the baseline subset selection described in [5] and the proposed fixed list as a function of N_{sat}.*

The reduction in computational load is very large for $P_{sat} = 10^{-3}$ (factor of 6 to almost 100), and still significant for 10^{-4} (factor of 2-3 to 5).

SUMMARY

Forming the list of subsets can be perceived as one of the most complex steps in the ARAIM airborne algorithm, especially with large P_{sat} values. This paper proposes to use the following fixed list of subsets for a dual constellation configuration:

- all-in-view (1 subset)
- single satellite out (N_{sat} subset)
- single constellation out (2 subsets)
- single constellation out and single satellite out (N_{sat} subsets)

This approach has two advantages: it simplifies the algorithm (the list of subsets is no longer dynamic), and it reduces the computational burden. For a baseline GPS – Galileo configuration with a P_{sat} of 10^{-3}, the number of subsets is reduced from several thousands to less than seventy with a minimal impact on availability.

ACKNOWLEDGEMENTS

This work was funded by the Federal Aviation Administration.

APPENDIX

An upper bound on the probability of two or more satellite faults is given by:

$$\sum_{i<k} P_{sat,i}^{(j)} P_{sat,k}^{(j)} \tag{11}$$

It can be shown that:

$$\sum_{i<k} P_{sat,i}^{(j)} P_{sat,k}^{(j)} = \frac{1}{2}\left\{\left(\sum_{i} P_{sat,i}^{(j)}\right)^2 - \left(\sum_{i} P_{sat,i}^{(j)2}\right)\right\} \quad (12)$$

REFERENCES

[1] Working Group C, ARAIM Technical Subgroup, Milestone 3 Report, February 26, 2016. Available at: http://www.gps.gov/policy/cooperation/europe/2016/working-group-c/

http://ec.europa.eu/growth/tools-databases/newsroom/cf/itemdetail.cfm?item_id=8690

[2] Gerbeth, Daniel, Martini, Ilaria, Rippl, Markus, Felux, Michael, "Satellite Selection Methodology for Horizontal Navigation and Integrity Algorithms," *Proceedings of the 29th International Technical Meeting of The Satellite Division of the Institute of Navigation (ION GNSS+ 2016)*, Portland, Oregon, September 2016, pp. 2789-2798.

[3] Walter, Todd, Blanch, Juan, and Kropp, Victoria. "Satellite Selection for Aviation Users of Multi-Constellation SBAS." *Inside GNSS November/December 2016*

[4] Walter, Todd, Blanch, Juan, Choi, Myung Jun, Reid, Tyler, Enge, Per, "Incorporating GLONASS into Aviation RAIM Receivers," *Proceedings of the 2013 International Technical Meeting of The Institute of Navigation*, San Diego, California, January 2013, pp. 239-249.

[5] Walter, T., Blanch, J., Enge, P., "Reduced Subset Analysis for Multi-Constellation ARAIM," *Proceedings of the 2014 International Technical Meeting of The Institute of Navigation*, San Diego, California, January 2014, pp. 89-98.

[6] Ge, Yishan & Wang, Zhipeng & Zhu, Yanbo. (2017). Reduced ARAIM monitoring subset method based on satellites in different orbital planes. GPS Solutions. 21. . 10.1007/s10291-017-0658-x.

[7] Orejas, Martin, Skalicky, Jakub, "Clustered ARAIM," *Proceedings of the 2016 International Technical Meeting of The Institute of Navigation*, Monterey, California, January 2016, pp. 224-230.

[8] Orejas, Martin, Skalicky, Jakub, Ziegler, Ute, "Implementation and Testing of Clustered ARAIM in a GPS/Galileo Receiver," *Proceedings of the 29th International Technical Meeting of The Satellite Division of the Institute of Navigation (ION GNSS+ 2016)*, Portland, Oregon, September 2016, pp. 1360-1367.

[9] Working Group C reference airborne ARAIM algorithm description document version 3, November 2017. Available upon request.